Reversible electron-transfer reactions within a nanoscale metal oxide cage mediated by metallic substrates

CHRISTOPHER FLEMING[1], DE-LIANG LONG[1], NICOLA McMILLAN[1], JACQUELINE JOHNSTON[1,4], NICOLAS BOVET[1], VIN DHANAK[2,3], NIKOLAJ GADEGAARD[4], PAUL KÖGERLER[5], LEROY CRONIN[1]* AND MALCOLM KADODWALA[1]*

[1]Department of Chemistry, The University of Glasgow, Glasgow G12 8QQ, UK
[2]Physics Department, University of Liverpool L69 3BX, UK
[3]CLRC Daresbury Laboratory, Warrington WA4 4AD, UK
[4]Department of Electronics and Electrical Engineering, University of Glasgow, Glasgow G12 8LT, UK
[5]Ames Laboratory and Department of Physics & Astronomy, Iowa State University, Ames, IA 50011, USA
*e-mail: malcolmk@chem.gla.ac.uk; L.Cronin@chem.gla.ac.uk

Published online: 30 March 2008; doi:10.1038/nnano.2008.66

Transition metal oxides exhibit a rich collection of electronic properties and have many practical applications in areas such as catalysis and ultra-high-density magnetic data storage. Therefore the development of switchable molecular transition metal oxides has potential for the engineering of single-molecule devices and nanoscale electronics. At present, the electronic properties of transition metal oxides can only be tailored through the irreversible introduction of dopant ions, modifying the electronic structure by either injecting electrons or core holes. Here we show that a molybdenum(VI) oxide 'polyoxometalate' molecular nanocluster containing two embedded redox agents is activated by a metallic surface and can reversibly interconvert between two electronic states. Upon thermal activation two electrons are ejected from the active sulphite anions and delocalized over the metal oxide cluster cage, switching it from a fully oxidized state to a two-electron reduced state along with the concomitant formation of an S–S bonding interaction between the two sulphur centres inside the cluster shell.

Polyoxometalate (POM) clusters are a large group of clusters with frameworks built from transition metal oxo anions linked by shared oxide ions[1]. Although POMs have much in common with bulk transition metal oxides (TMOs), their molecular nature means they have a vast structural diversity[2], with many applications in areas such as catalysis[3] and materials science[4–7]. POM clusters are extraordinary molecules, because they have a high charge, are of nanoscale dimensions, and the framework cage can encapsulate many types of small templates. The potential to incorporate guests to dope the oxide cage is of great interest, because the electronic properties of the cluster could be manipulated using these internal guests[8]. In POMs, the use of oxo-anion guests based upon main group elements (such as phosphorus or sulphur) is required to template the cluster cage[9]. For instance, the Dawson cluster, a frequently studied structure type with 18 metal ions (either molybdenum or tungsten) and an elliptical shape, encapsulates two 'load-bearing' tetrahedral anions such as sulphate ($S^{VI}O_4^{2-}$) or phosphate ($P^{V}O_4^{3-}$), which are vital for retaining the structural integrity of the cluster, but are normally chemically inert. If these inert templates could be replaced with electronically active templates[9], then we have hypothesized that this would open the way to the design of molecular TMOs exhibiting properties not observed in their bulk analogues: for example, allowing the engineering of single-molecule electronic devices[10].

It may be possible to encapsulate dopants that can reversibly dope the cage without causing a bulk structural change, because of their encapsulation. To explore this concept we tailored a molecular functionalized molybdenum(VI) oxide (POM) molecular cluster ($\mathbf{1} = \beta\text{-}[Mo_{18}O_{54}(SO_3)_2]^{4-}$), containing two 'templating' sulphite anions, which are positioned 0.33 nm ($S\cdots S$) apart within the cluster shell (Fig. 1), thereby aiming to stimulate the formation of a S–S bond, and releasing two electrons to the cluster shell[11].

As we have shown in earlier work[9], the $[\{Mo^{VI}O_3\}_{18}(S^{IV}O_3)_2]^{4-}$ cluster displays thermochromic behaviour and extensive redox chemistry[12], but it does not undergo the reversible intramolecular redox process in either solution or the solid state. In an attempt to elucidate if nanocluster **1** can be 'pushed' into a complete intramolecular redox reaction by radically changing the surrounding environment (that is, by removing the molecule cluster from the crystal lattice or solvated solution phase and placing isolated molecules on a highly polarizable metallic substrate), we have studied single monolayers of **1** on a range of surfaces. Experiments with monolayers of **1** on a gold surface demonstrate that this cluster has the unprecedented ability to reversibly interconvert between two distinct electronic states. In this process the $\{Mo_{18}O_{54}\}$ oxide shell, which encapsulates two pyramidal sulphite ($S^{IV}O_3^{2-}$) groups, is transformed from a fully oxidized

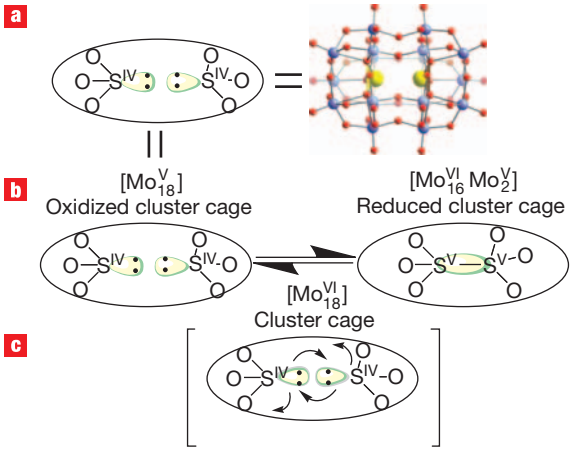

Figure 1 Schematic of the reversible S–S bond formation and electronic reorganization within the cluster cage. a, The $\{Mo_{18}O_{54}(SO_3)_2\}$ cluster framework is shown at the right, with the Mo atoms shown in blue, the oxygen atoms in red and the two sulphur atoms in yellow. This is abbreviated to the ellipse containing the two SO_3 groups at the left. **b**, The left ellipse represents the starting state for the fully oxidized cluster and the right ellipse represents the reduced state where the formation of the single S–S bond results in the movement of two electrons from the S atoms to the cluster cage, yielding $[\{Mo^{V}_{2}Mo^{VI}_{16}O_{54}\}\ (S^{V}_{2}O_6)]^{4-}$. **c**, Transition state, in which the four electrons (depicted by the arrows) rearrange, with two electrons forming the S–S bond, and the remaining two reducing the cluster shell.

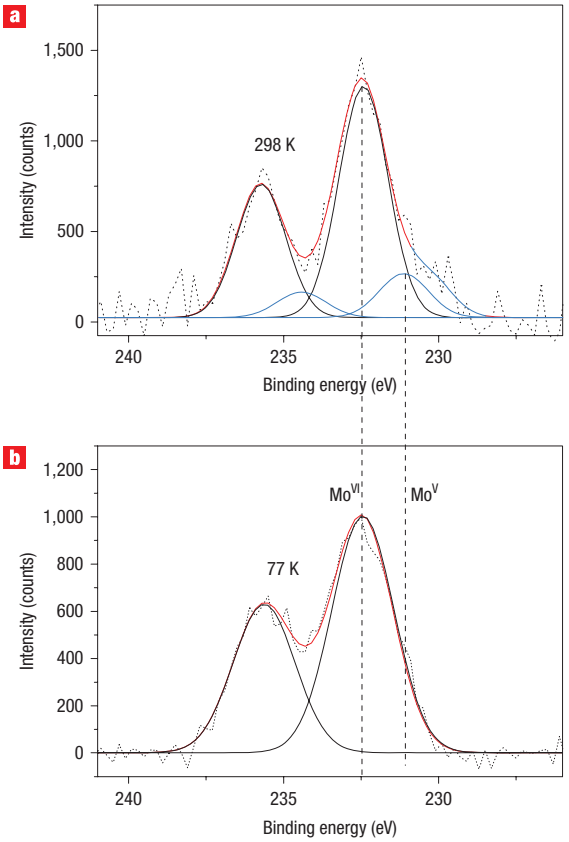

Figure 2 Mo 3*d* core-level spectra for cluster 1. a,**b**, Spectra at 298 K (**a**) and 77 K (**b**). The red lines show the appearance of bands associated with Mo^{V} at 298 K. The vertical dotted lines indicate the expected positions for Mo(VI) and Mo(V)[16]. The fitted curves are shown in blue and the shoulder that develops at 298 K is highlighted in thick blue.

state at 77 K $\{Mo^{IV}_{18}\}$ to a two-electron reduced mixed-valence state at 298 K $\{Mo^{IV}_{16}Mo^{V}_{2}\}$, and the reversibility of the process was demonstrated by a cycle of measurements from 298 K to 77 K to 298 K. This reversible electron transfer is commensurate with the formation of a bonded interaction between the two internal sulphite groups at 298 K. This is a thermally controlled process, which is activated by the induced local electric field associated with the image charge generated on the metal surface as a result of adsorbing **1**. The formation of the S–S bonded interaction results in the generation of a new populated electronic state in the bandgap of the oxide cluster molecule, which can be compared to a traditional insulator-to-metal transition, yet without a gross structural change in the bulk because the changes are confined to the molecular cage. This molecular metal oxide can therefore be regarded as a new type of molecular transport switch[13], which is thermally driven and activated by the local electrical field associated with an image charge generated in the metallic surface.

We chose a nanoscale molecular cluster with a $\{Mo^{VI}_{18}O_{54}\}$ shell encapsulating charge-bearing anions, which has an interior cavity large enough to include two active sulphite $(S^{IV}O_3)^{2-}$ anions. These anions are electronically interesting, because the sulphur atoms are in an intermediate oxidation state and possess a vacant coordination site, a lone pair of electrons, and can change oxidation state and coordination number; this is in contrast to templates such as SO_4^{2-} and PO_4^{3-}, which are chemically inert.

The key to the activation of the cluster arises from the precise positioning of the S centres of the sulphite anions within the cluster cage; these are located 3.29 Å apart, a close separation in chemical terms as this distance is 0.4 Å less than the sum of the sulphur van der Waals radii, yet is longer than the 2.15 Å S–S bond in a complexed dithionate-like anion $(O_3S–SO_3^{2-})$, which would result from the reaction of two sulphite anions along with the loss of two electrons, and thus provides a barrier to spontaneous bond formation. Consequently, if the sulphite groups could be pushed together through thermally activated vibrations, the possibility of reversible S–S bond formation arises, with a commensurate transfer of two electrons onto the cluster cage. This reversible intramolecular redox reaction is depicted in Fig. 1.

For comparison, and as a structural control, we also studied monolayers[14] of the conventional analogous sulphate-based Dawson anion $[\{Mo^{VI}_{18}O_{54}\}(S^{VI}O_4)_2]^{4-}$ (**2**). This control cluster is important, because it is chemically as reactive as **1** (in fact it is easier to electrochemically reduce **2** than **1** and both clusters have the same charge), but it contains an inert cluster core[12]. The temperature dependence (at 298 K and 77 K) of the valence-level electronic structure of the cluster layers was examined using valence-level photoemission spectroscopy[15], and the oxidation state of the Mo centres was monitored with core-level X-ray photoelectron spectroscopy (XPS). Both XPS and valence photoemission measurements were performed with the samples in an ultrahigh-vacuum environment ($P < 1 \times 10^{-9}$ mbar). Control **2** did not show significant changes as a function of temperature, but **1** exhibited electronic changes as a function of temperature that are consistent with the reversible intramolecular redox process illustrated in Fig. 1.

Figure 2 shows the spectrum of **1** at 77 K for which, like the control sample **2**, the data collected can be fitted to a single pair of 3*d* peaks with binding energies of 232.5 and 235.6 eV, respectively,

demonstrating that the Mo ions in these clusters under these conditions exist as fully oxidized Mo(VI) ions, therefore indicating that the clusters are fully oxidized[16]. However, the Mo 3*d* spectrum of the **1** layer at 298 K can only be fitted satisfactorily with two pairs of 3*d* components. The major component ($86 \pm 4\%$) is the Mo(VI); the second minor components ($14 \pm 4\%$) have $d^{5/2}$ and $d^{3/2}$ binding energies of 230.5 and 233.6 eV, respectively, characteristic of the reduced Mo(V). This shows that heating cluster **1** to 298 K from 77 K causes the reduction of the cluster shell by approximately 2 electrons[17], whereas **2** remains unchanged (see Supplementary Information).

Crucially, the same temperature-dependent behaviour is also seen in the valence region of the photoemission spectra of cluster **1** (see Supplementary Information, Fig. S3) at cryogenic and room temperatures; the difference spectrum for the **1** species is shown in Fig. 3. This shares a common feature at 31.1 eV with the sulphate cluster control spectra (Fig. 3b), which is not seen in the cryogenic cluster spectrum of **1**.

The bands observed at 3.5 and 6.3 eV in the cluster difference spectra of compound **1** are in a similar region to those observed in previous photoemission studies of bulk samples of MoO_2, MoO_3, mixed Mo(IV) and Mo(VI) oxides and non-stoichiometric (defective) oxides[18]. This region is well reproduced by three gaussian components with binding energies of 2.6, 3.7 and 6.6 eV (see Supplementary Information). Based on assignments from previous work, the components at 3.7 and 6.6 eV are associated with electronic states of the bridging and terminal oxygen of the Mo oxide cage, and the component at 2.6 eV can be attributed to a Mo $4d^1$ electron, consistent with the Mo(V) component in the core-level spectrum. Clearly, the cluster monolayer of compound **1** is partially reduced at room temperature, and the presence of the 3.7 and 6.6 eV components in the difference spectra reflects a change in the electron distribution of the clusters due to the reduction of Mo(VI) to Mo(V). Complementing these findings, the peaks at 12.1, 16.7, 22.3 and 31.1 eV observed in the cluster difference spectrum of **1** (Fig. 3a) are indicative[19,20] of an oxidized, tetrahedral sulphur-based species, supporting the suggestion that the encapsulated sulphite groups in the cluster have undergone oxidation to form a dithionate-like anion in which the two sulphur atoms occupy a tetrahedral geometry; the electrons for the reduction of the Mo centres are thus not provided by the Au surface. Further evidence for the reduction of the cluster cage **1** by the internal sulphite anions rather than an external reducing agent such as the metallic substrate or another entity is provided by the fact it is harder to reduce **1** than the control cluster **2** by ~100 mV (ref. 12). Therefore, reduction from an external species would also reduce the control cluster **2**, and this is not observed. Importantly, studies on an isomer of **1** (where the orientation of the sulphite ions with respect to the cluster shell is different; see Supplementary Information) have shown that it is not as active as **1**, and this also demonstrates the precise control of the orientation of the sulphite groups that is required to engineer the functional cluster.

The electronic effects underpinning the observed electronic changes were modelled with density functional theory (DFT) calculations, from which we identified a potential mechanism explaining the tendency of the observed changes. We found that adding a single reaction coordinate by shifting the two S centres each by a displacement Δx (to simulate the effects of thermal activation), and the oxo positions belonging to the sulphite groups by $\Delta x/2$ towards each other (along the main symmetry axis of the cluster anion, **1**), did not induce a concerted intramolecular electron transfer coupled to the formation of an S–S single bond in the gas phase. However, if mirror charges that are induced in the highly polarizable metallic Au surface by the cluster anion were modelled by a rectangular set of four single positive charges on one (arbitrary) side of the fourfold negative cluster anion structure (Fig. 4), a decrease in the S–S distance to ~2.3 Å indeed caused the formation of a bonding overlap and a partial reduction of the molybdate cluster shell.

This stabilizing mirror charge effect appears to play an important role in the observed surface activation, because such a displacement of the sulphur centres relative to the molybdate cluster shell can, in principle, be caused by thermal vibrations. Therefore the adsorption of **1** onto a metallic Au substrate would

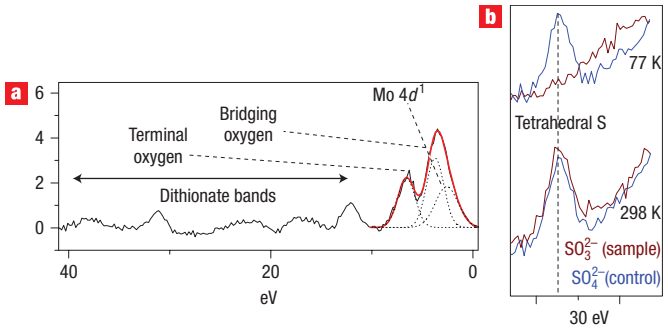

Figure 3 Photoemission spectra of cluster 1. a, The difference spectra (298 K–77 K) for cluster **1** in the valence region. Bands associated with the reduced Mo ions[18] and the formation of $[O_3S{-}SO_3]^{2-}$ (dithionate-like anion) are observed at 12.1, 16.7, 22.3 and 31.1 eV. The three peaks at 2.7, 3.5 and 6.3 eV can be fitted with three gaussians (smooth grey curves) at 2.6 (assigned to the Mo $4d^1$), 3.7 and 6.6 eV to give an overall envelope shown in red. **b**, Region centred around 30 eV in the photoemission spectra for the control (**2**) and sample (**1**) covering the region characteristic for tetrahedral sulphur[19]. A common peak at 31.1 eV is seen in both the control compound **2** at 298 and 77 K (blue line) and then appears in the spectra of **1** (brown line) at 298 K, showing the reversible development of a tetrahedral sulphur centre in cluster **1**.

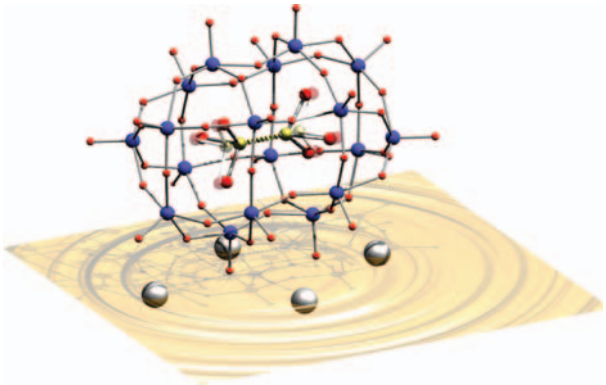

Figure 4 Depiction of cluster 1 on a Au surface, generating an image charge. Scheme of the displacement model reaction used for DFT simulations in the presence of an array of point charges (silver spheres) that are situated in the Au surface (orange plane). The sulphite S (yellow spheres) and O (large red spheres) centres are shifted towards each other within the $\{Mo_{18}\}$ Dawson cluster shell (Mo: small blue spheres; O: small red spheres) until a bonding S···S interaction is formed. Original S/O positions are shown as semitransparent spheres for the spanned trigonal pyramid. Note that the oxo positions are only shifted by half of the displacement Δx of the S positions.

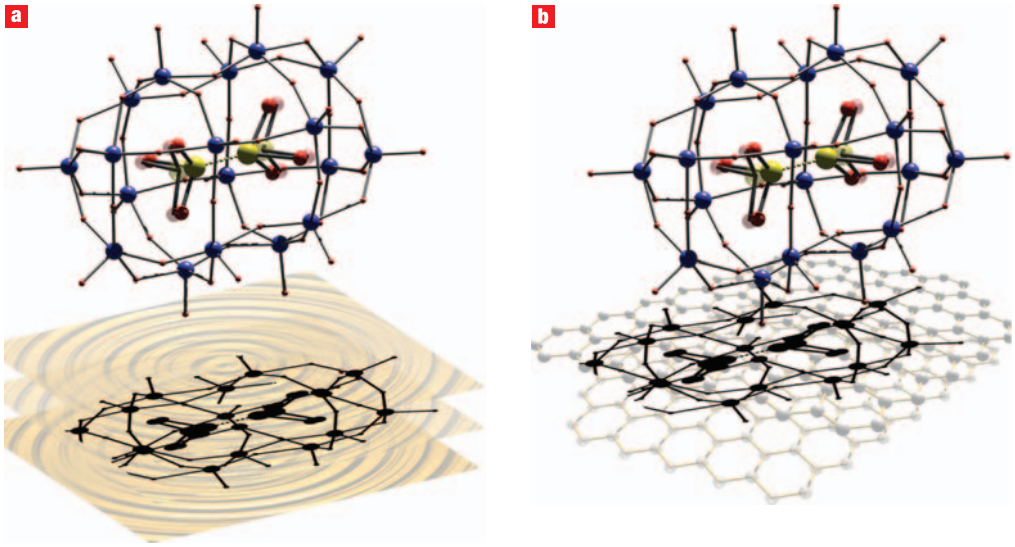

Figure 5 Evolution of the image charge from the cluster on Au and HOPG. a,**b**, Scheme depicting the development of the image charge (black image) that develops when the cluster (colour scheme as in Fig. 4) is adsorbed on the surface Au (**a**) and HOPG (**b**). On Au the image charge will develop within the surface at a distance that mirrors the distance between the cluster and the surface. However, on HOPG the image charge will be confined to the top graphene layer so the field will be larger for HOPG than Au.

appear to facilitate a stronger interaction between the encapsulated sulphite anions, resulting in the formation of a dithionate-like anion and the release of two electrons that reduce the Mo(VI) centres, as depicted in Fig. 1. Furthermore, examination of this effect as a function of the precise orientation of the sulphite anions within cluster **1** demonstrates that this reversible electron transfer is also dependent on the orientation of the sulphite anions within. This study allows us to prove that the reversible reduction of cluster **1** is due to an internal rearrangement and not due to another process, such as cluster decomposition or the introduction of another oxo species, because all three cluster cages would also be equally susceptible to such transformations[11,12].

To explore further the nature of the surface field effect that appears to activate or induce this thermally driven process, we conducted additional surface XPS experiments with **1** and **2** on a number of substrates—first on an Au surface coated with a monolayer of cysteine and second on highly orientated pyrolytic graphite (HOPG). These experiments showed that neither cluster undergoes any process on the cysteine-coated gold, yet **1** is activated even at room temperature when adsorbed onto HOPG (see Supplementary Information, Fig. S7) and is pushed to an irreversible state compared to compound **1** on gold. Crucially, the sulphate-based control **2** (which is easier to reduce than the sulphite-based cage **1**) does not show any change. Therefore we can unambiguously state that the surface effect is real and the rapid promotion of the process by HOPG is a result of the image charge being localized within the surface graphene sheet, which means that the separation between the cluster and the induced charge is shorter than for the Au substrate, where the cluster and the image charge will be equidistant from the surface (Fig. 5). This results in the local field felt by the S atoms within the cluster cage being much higher on HOPG than on Au (Fig. 5). This higher local field results in the activation of the sulphite-containing cluster **2**, even at room temperature, and the XPS studies show the formation of Mo(V) and metallic Mo(0) (this behaviour is shown by **1** on Au when heated to decomposition at ~500 K). Although it has been previously shown that POM clusters can adsorb strongly onto HOPG (ref. 21), the present result is remarkable, because the control studies demonstrate that the HOPG induces an internal rearrangement without directly transferring charge to the cluster (otherwise the control would itself be reduced as it is easier to reduce than the active cluster).

In summary we have demonstrated that adsorption of molecular TMOs (containing sulphite anions encapsulated and precisely oriented within the cluster cage) onto Au films promotes a reversible intramolecular redox reaction that effectively injects electrons into a nanoscale Mo(VI) oxide shell. Therefore, this process, through a reduction reaction, introduces Mo(V) dopants into the system, which radically changes the oxide's electronic structure and is reversible because the reaction is confined inside the cluster shell, like a ship-in-a-bottle; this thermally controlled process is effectively activated by the field associated with the metallic surface.

Observation of this new phenomenon is important for several reasons. First, it represents a transition from an insulating to a more metal-like state in a molecular oxide that proceeds without a gross structural change; such processes are rarely observed in solid-state materials, and the reversible mechanism presented is unprecedented[20–22]. Second, the metallic surface clearly mediates the intramolecular redox process[23] by allowing the generation of image charges, which generate an electrostatic field that penetrates the cluster sheath and facilitates bonding between the two sulphite groups, causing the transfer of two electrons to the metal oxide shell. The observation of the rapid promotion of this process within the metal oxide cluster by HOPG has possible implications for the use of metal oxide clusters on HOPG/graphene surfaces in the generation of hybrid carbon–POM electronic devices. Further work will be done to explore both electronic and optical routes to developing POM clusters, the fabrication of devices, as well as to expand the theoretical analysis to more realistically model how the electronic structure of the cluster is affected by the surface[24].

METHODS

PHOTOEMISSION

All experiments were performed at the Central Laboratories of the Research Councils (CLRC) laboratory at Daresbury, at station 4.1 of the Synchrotron Radiation Source (SRS). This station has been described in detail elsewhere[15]. It includes an UHV beamline with a spherical grating monochromator, which provided photons in the 14–170 eV range. The UHV endstation was equipped with a CLAM 2 (VG) concentric hemispherical analyser and an X-ray source (Al Kα) for XPS analysis. Electron bombardment heating was used on the samples and temperature was monitored either with an optical pyrometer (elevated temperatures) or a chromel alumel thermocouple (cyrogenic temperature ~140 K). The valence-region photoemission measurements were collected using photon energies of 140 eV, and all binding energies were referenced to E_F. Valence-region spectra were collected in normal emission geometry with the photon beam incident at 55° (with respect to the surface normal). Core-level spectra (C(1*s*), O(1*s*) and Mo (3*d*)) were collected at normal emission using a Al Kα source, the X-rays from which were incident at 73° with respect to the surface normal.

SAMPLE PREPARATION

Samples were prepared by dipping polycrystalline Au films in 1 mM of the HPOM solutions in MeCN. After immersion, the samples were dried in a stream of nitrogen gas. This method has been applied by Barteau and co-workers on other POM systems and has been found to produce single monolayers[14].

COMPUTATION DETAILS

DFT calculations (including Löwdin and Mulliken population analysis) using the TURBOMOLE 5.7 package required TZVPP basis sets and hybrid B3-LYP exchange-correlation functionals to converge. All structures (C_1 symmetry) were allowed to briefly equilibrate until a small, consistent mean energy gradient $|dE/dxyz|$ was reached. The mean shift for each atomic position generated by the free geometric equilibration amounted to 0.007 Å. See Supplementary Information for full details.

Received 18 October 2007; accepted 28 February 2008; published 30 March 2008.

References

1. Long, D.-L., Burkholder, E. & Cronin, L. Polyoxometalate clusters, nanostructures and materials: From self assembly to designer materials and devices. *Chem. Soc. Rev.* **36,** 105–121 (2007).
2. Müller, A., Shah, S. Q. N., Bögge, H. & Schmidtmann, M. Molecular growth from a Mo_{176} to a Mo_{248} cluster. *Nature* **397,** 48–50 (1999).
3. Rhule, J. T. *et al.* Stable, self-assembling, equilibrating catalysts for green chemistry. *J. Am. Chem. Soc.* **123,** 12101–12102 (2001).
4. Long, D.-L. & Cronin, L. Towards polyoxometalate-integrated nano systems. *Chem. Eur. J.* **12,** 3698–3706 (2006).
5. Song, Y.-F. *et al.* Design of hydrophobic polyoxometalate hybrid assemblies beyond surfactant encapsulation. *Chem. Eur. J.* **14,** 2349–2354 (2008).
6. Song, Y.-F., Long, D.-L. & Cronin, L. Non covalently connected frameworks with nanoscale channels assembled from a tethered polyoxometalate–pyrene hybrid. *Angew. Chem. Int. Edn* **46,** 3900–3904 (2007).
7. Song, Y.-F. *et al.* From polyoxometalate building blocks to polymers and materials: The silver connection. *J. Mater Chem.* **17,** 1903–1908 (2007).
8. Long, D.-L., Streb, C., Song, Y.-F., Mitchell, S. & Cronin, L. Unravelling the complexities of polyoxometalates in solution using mass spectrometry: Protonation versus heteroatom inclusion. *J. Am. Chem. Soc.* **130,** 1830–1832 (2008).
9. Long, D.-L., Kögerler, P. & Cronin, L. Old clusters with new tricks: Engineering S···S interactions and novel physical properties in sulphite-based Dawson clusters. *Angew. Chem. Int. Edn* **43,** 1817–1820 (2004).
10. Lewis, P. A. *et al.* Molecular engineering of the polarity and interactions of molecular electronic switches. *J. Am. Chem. Soc.* **127,** 17421–17426 (2005).
11. Long, D.-L., Abbas, H., Kögerler, P. & Cronin, L. Confined electron-transfer reactions within a molecular metal oxide 'Trojan Horse'. *Angew. Chem. Int. Edn* **44,** 3415–3419 (2005).
12. Baffert, C. *et al.* Experimental and theoretical investigations of the sulfite-based polyoxometalate cluster redox series: α- and β-$[Mo_{18}O_{54}(SO_3)_2]^{4-/5-/6-}$. *Chem. Eur. J.* **33,** 8472–8433 (2006).
13. Badjić, J. D., Balzani, V., Credi, A., Silvi, S. & Stoddart, J. F. A molecular elevator. *Science* **303,** 1845–1849 (2004).
14. Song, I. K., Kaba, M. S. & Barteau, M. A., Nanoscale investigation of mixed arrays of Keggin-type and Wells–Dawson-type heteropolyacids (HPAs) by scanning tunnelling microscopy (STM). *Langmuir* **18,** 2358–2362 (2002).
15. Dhanak, V. R., Robinson, A. W., van der Laan, G. & Thornton, G. Beamline 4: A dedicated surface science facility at Daresbury Laboratory. *Rev. Sci. Instrum.* **63,** 1342–1345 (1992).
16. Werfel, F. & Minni, E. Photoemission study of the electronic structure of Mo and Mo oxides. *J. Phys. C* **16,** 6091–6100 (1983).
17. Mo(V) has a characteristic $3d^{5/2}$ binding energy of 230.7 eV. Available at NIST Photoelectron spectroscopy database: http://srdata.nist.gov/xps/.
18. Tokarz-Sobieraj, R. *et al.* Properties of oxygen sites at the MoO_3(010) surface: Density functional theory cluster studies and photoemission experiments. *Surf. Sci.* **489,** 107–125 (2001).
19. Audi, A. A. & Sherwood, P. M. A. X-ray photoelectron spectroscopic studies of sulfates and bisulfates interpreted by Xα and band structure calculations. *Surf. Interface Anal.* **29,** 265–275 (2000).
20. Adler, D. Mechanisms for metal-non metal transitions in transition-metal oxides and sulfides. *Rev. Mod. Phys.* **40,** 714–736 (1968).
21. Kuhn, N. & Anson, F. C. Adsorption of monolayers of $\{P_2Mo_{18}O_{62}\}^{6-}$ and deposition of multiple layers of $\{Os(bpy)_3\}^{2+}$ – $\{P_2Mo_{18}O_{62}\}^{6-}$ on electrode surfaces. *Langmuir* **12,** 4008–4014 (1996).
22. Imada, M., Fujimori, A. & Tokura, Y. Metal–insulator transitions. *Rev. Mod. Phys.* **70,** 1039–1263 (1998).
23. Rohmer, M. M. & Bénard, M. Bond-stretch isomerism in strained inorganic molecules and in transition metal complexes: A revival? *Chem. Soc. Rev.* **30,** 340–354 (2001).
24. Lehmann, J., Gaita-Arino, A., Coronado, E. & Loss, D. Spin qubits with electrically gated polyoxometalate molecules. *Nature Nanotech.* **2,** 312–317 (2007).

Acknowledgements

The authors would like to thank the Leverhulme Trust (London), the Royal Society, the University of Glasgow, WestCHEM and the Engineering and Physical Sciences Research Council (UK) for funding. Correspondence and requests for materials should be addressed to M.K. and L.C. Supplementary information accompanies this paper on www.nature.com/naturenanotechnology.

Author contributions

L.C. and M.K. conceived and designed the experiments, D.L. synthesized the clusters and N.G., N.M. and J.J. prepared the samples for the photoemission studies. C.F. and J.J. performed the experiments, M.K., C.F. and J.J. analysed the photoemission data, and N.B. and V.D. helped with the synchrotron experiments. P.K. performed the theoretical calculations. M.K. and L.C. co-wrote the paper.